Signal-to-noise-ratio equations for a heterodyne laser radar

Charles A. DiMarzio and Scott C. Lindberg

We analyze the signal-to-noise-ratio equations for a heterodyne laser radar with identical transmit and receive optics. We defines the beam-profile efficiency, a quantity that must be maximized to optimize a system design. This calculation can be used to evaluate a system in both near and far fields for focused and nonfocused systems. The beam-profile efficiency can be evaluated in many ways, and we describe one possible solution. Using this solution, we present the results of an actual system evaluation.

Introduction

To obtain information about the velocity of a target by using laser radar, we must employ a coherent mixing or heterodyne technique in which the phase of a scattered signal is compared with the phase of a stable reference signal. For this measurement, both the total energy received and the coherence of the received signal are important to optimize signal processing. In this paper we present a calculation of the heterodyne signal-to-noise ratio expected from a group of complex scatterers, most often the atmosphere. The effects of atmospheric turbulence are neglected in this discussion.

Signal-to-Noise Ratio

The signal-to-noise ratio (SNR) for a coherent laser radar with a shot-noise-limited detector is given by[1]

$$\mathrm{SNR} = [\eta PF]/[h\nu B], \tag{1}$$

where η includes all system losses and the quantum efficiency of the detector, P is the optical power transmitted by the system, $h\nu$ is the energy of a photon, B is the i.f. bandwidth of the receiver, and F is a quantity that describes the heterodyning of the transmitter and local oscillator.

For an area target, we can express the quantity F in terms of a quantity S, which is independent of the target:

$$F = S\rho(\pi), \tag{2}$$

where S is the sensitivity of the system and $\rho(\pi)$ is the reflectivity of the target. The sensitivity, equivalent to the responsitivity,[2] $C(R)$ of the coherent laser radar, is described

$$S = \lambda^2 \int\int \frac{I_t}{P_t}\frac{I_r}{P_r}\,\mathrm{d}x\mathrm{d}y, \tag{3}$$

where λ is the wavelength, the I terms are the irradiances of the transmitter and the backpropagated local oscillator (BPLO) beams at the target, and the P terms are the corresponding powers. The BPLO is the virtual beam coming from the target that would produce the same wave front at the detector as the actual local oscillator. It is customary to consider P_t as the power of the transmitter prior to truncation, because the truncation must be considered in optimizing S. Likewise, P_r is usually the total power incident on the detector, because this power contributes to the noise. Various schemes for matching the BPLO to the truncation of the system's aperture stop are possible,[3] but these may prove difficult to implement in practice. In the present study, P_r is the total local oscillator power in the beam at it comes from the laser.

For a volumetric target, F is determined by integrating the sensitivity over the volume of target so that

$$F = \beta(\pi)\int S\mathrm{d}z, \tag{4}$$

where $\beta(\pi)$ is the atmospheric-backscatter coefficient.

The SNR for a variety of systems has been obtained by modeling the system with an aperture size D as matched Gaussian beams of diameter D.[4] The essence of the result is

$$S_{SH}(R) = \lambda^2/[\pi w_{SH}{}^2(R)] \tag{5}$$

The authors are with the Center for Electromagnetics Research, Northeastern University, 360 Huntington Avenue, Boston, Massachusetts 02115.

Received 11 September 1991.
0003-6935/92/214240-07$05.00/0.

and is determined for perfectly matched, perfectly overlapping Gaussian beams of diameter $2w_{SH}(R)$ at the target, where R is the range of the target from the aperture. The Gaussian beam diameter at the aperture is chosen to be equivalent to the aperture diameter, i.e., $w_{SH}(0) = D/2$. The Gaussian beam diameter at any range is determined by the usual equations for Gaussian beam propagation. At the far field of a collimated system or at the focus of a focused system,

$$S_{SH}(R) = [\pi D^2]/[4R^2] \tag{6}$$

is equivalent to $D_{\max}(R)$, which is the maximum direct responsitivity for a given aperture, and is equal to $D(R)/T_T$, where $D(R)$ is the direct responsitivity[2] and T_T is the fraction of the transmitter power to pass through the transmitter aperture.[3] In the near field, the equivalence does not hold as $D(R) = [\pi D^2]/[4R^2]$ approaches infinity. The actual expression for $D(R)$ becomes complicated in the near field because the field of view of the detector is greatly reduced.

There is much confusion over the term "heterodyne efficiency." The heterodyne efficiency defined as[2]

$$\eta_H(R) = C(R)/D(R) \tag{7}$$

is the fraction of the direct-detection power converted to coherent-detection power. If $\eta_H(R)$ were optimized in a system design, the process would not necessarily maximize $C(R)$, because $\eta_H(R)$ does not take into account the truncation of the transmitter at the aperture. We could optimize $\eta_H(R)$ by minimizing $D(R)$, but this would minimize the direct-detection power. Obviously this minimization would not provide an optimum system design. In reality, it is necessary to maximize $S = C(R)$ to optimize a system design. S is related to $S_{SH}(R)$ such that $S = \eta_{BP}(R)S_{SH}(R)$, where $\eta_{BP}(R)$ is the beam-profile efficiency as given by

$$\eta_{BP}(R) = \pi w_{SH}^2(R) \iint \frac{I_t}{P_t}\frac{I_r}{P_r}\,dxdy, \tag{8}$$

and both $w_{SH}(R)$ and $S_{SH}(R)$ are determined uniquely by the aperture size and range.

In the far field,

$$2w_{SH}(R) = [4\lambda R]/[\pi D], \tag{9}$$

and $\eta_{BP}(R)$ is equivalent to the system-antenna efficiency η_s as given by[3]

$$\eta_s = \left(\frac{2\lambda R}{\sqrt{\pi}D}\right)^2 \iint \frac{I_t}{P_t}\frac{I_r}{P_r}\,dxdy. \tag{10}$$

This equation can be used to determine the beam-profile efficiency in the far field or at the focus, whereas the general expression in Eq. (8) must be used at other ranges. A system can be optimized by maximizing either $\eta_{BP}(R)$ or η_s. The beam-profile efficiency can be evaluated in a number of ways, including using Fresnel–Kirchhoff integrals or expanding the laser-beam profile as a (possibly infinite) sum of orthogonal functions.[5] Figure 1 is a summary of the various quantities of interest.

Hermite–Gaussian Expansion

When determining the beam-profile efficiency by expanding each laser-beam profile with orthogonal functions, we can use any set of orthogonal functions. For this example, the expansion will be done using Hermite–Gaussian functions. A set of beam coefficients can be determined for each laser from the expansion. From these beam coefficients the beam-profile efficiency can be determined for any range from the system, and an evaluation of the expected SNR can be made.[1]

The Hermite–Gaussian functions converted to our notation are given by[6]

$$h_{mn}(x, y) = h_m(x)h_n(y),$$
$$h_m(x) = (2/\pi)^{1/4}(2^m m!w)^{-1/2} \times H_m(\sqrt{2}x/w)\exp(-x^2/2w^2), \tag{11}$$

where $H_m(\alpha)$ is the Hermite polynomial.[7]

The beam coefficients at the lasers are computed for the transmitter using

$$A_{mn} = \iint E_t(x_1, y_1, z_1)h_{mn}(x_1, y_1)dx_1dy_1, \tag{12}$$

and for the reference

$$B_{mn} = \iint E_r(x_1, y_1, z_1)h_{mn}(x_1, y_1)dx_1dy_1. \tag{13}$$

To determine the beam profile at a particular range, we must make phase changes to the beam coefficients. The phase change is

$$\psi_{mn} = (1 + m + n)\tan^{-1}(z/b), \tag{14}$$

and the beam-field amplitude profile at any range can

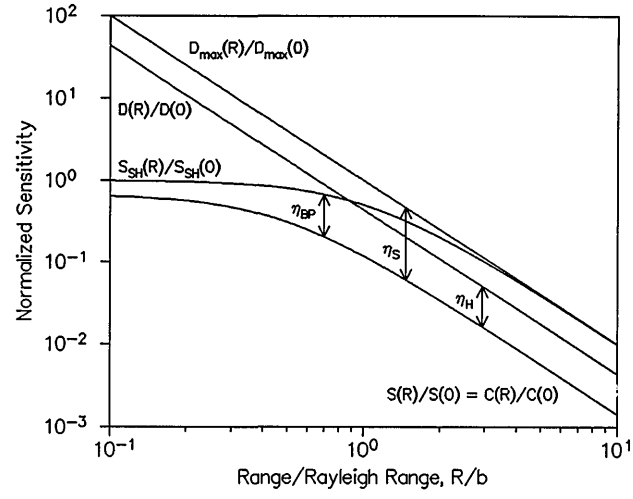

Fig. 1. Summary of various quantities of interest graphed as functions of R/b, where R is the range of the target and b is the Rayleigh range, including sensitivities [$D_{\max}(R)$, $D(R)$, $S_{SH}(R)$, $S(R)$] and efficiencies [η_{BP}, η_H, η_S].

be obtained as

$$E_t(x_2, y_2, z_2) = \sum_m \sum_n A_{mn} h_{mn}(x_2, y_2) \exp[\psi_{mn}(z_2)] \tag{15}$$

for the transmitter beam and similarly for the reference beam.

For computational purposes we use dimensionless-length units, so the irradiances are functions of $x/w_{\mathrm{ref}}(R)$ and $y/w_{\mathrm{ref}}(R)$, where $w_{\mathrm{ref}}(R)$ is the Gaussian beam radius at the target chosen for the Hermite–Gaussian functions. We choose $w_{\mathrm{ref}}(R)$ to put the most power in the 00 mode. The beam-profile efficiency becomes

$$\eta_{\mathrm{BP}}(R) = \left| \frac{2\lambda R}{\sqrt{\pi} D w_{\mathrm{ref}}(R)} \right|^2 \frac{\iint I_t I_r \mathrm{d}x' \mathrm{d}y'}{\iint I_t \mathrm{d}x' \mathrm{d}y' \iint I_r \mathrm{d}x' \mathrm{d}y'}. \tag{16}$$

Assuming unit power in both beams and letting $w_{\mathrm{ref}}(R) = \lambda R/[\pi w_{\mathrm{ref}}(0)]$ at the target, we find that the equation only in the far field or at the focus becomes

$$\eta_{\mathrm{BP}}(R) = \frac{\pi w_{\mathrm{ref}}^2(0)}{r_{\mathrm{ap}}^2} \iint I_t I_r \mathrm{d}x' \mathrm{d}y', \tag{17}$$

where $w_{\mathrm{ref}}(0)$ is the Hermite–Gaussian function radius at the aperture and r_{ap} is the aperture radius. This equation is solved by replacing the irradiances with the appropriate results from Eq. (15). Equation (17) can be modified to be appropriate for any range by replacing $w_{\mathrm{ref}}^2(0)/r_{\mathrm{ap}}^2$ with $w_{SH}^2(R)/w_{\mathrm{ref}}^2(R)$.

System Analysis

The computation was compared with experimental results from a short-range, cw system. For this system, the transmitter and reference lasers of the laser radar are CO_2-waveguide lasers with cosine-beam profiles:

$$E(x, y) = \cos[[\pi x]/[2w]] \cos[[\pi y]/[2w]]/w, \tag{18}$$

where $2w$ is the square-bore width. A particular problem of the system is a wire placed before the telescope. This wire is used to reduce the narcissus signal, which is a common problem in cw laser radars. The secondary of the telescope is designed to focus the narcissus onto this wire and reduce the signal generated by its mixing with the local oscillator. However, the wire has the effect of reducing the SNR of the system.

Figure 2 shows the optical layout of the laser radar. In the experiment, transmitter-beam profiles were taken at various ranges after the primary lens of the optical system. To compare the experimental results with the results from the Hermite–Gaussian

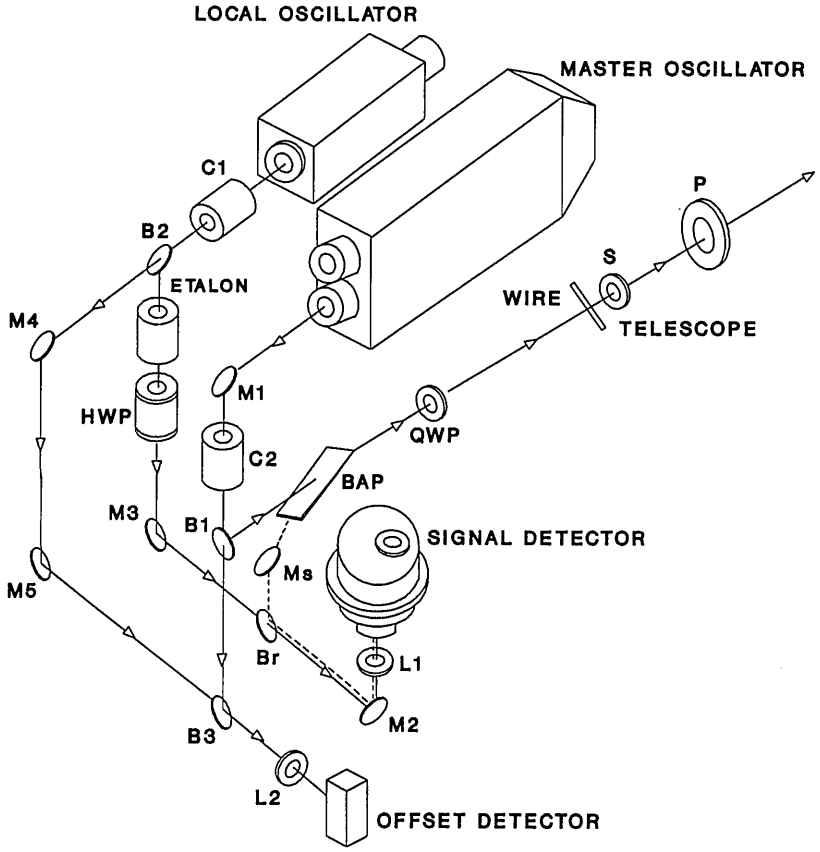

Fig. 2. Optical layout of the laser radar system. Of particular interest is the wire and the telescope consisting of the secondary, S, and the primary, P: BAP, Brewster-angle plate; B1–B3, beam splitters; C1, C2, collimators; HWP, half-wave plate; L1, L2, lenses; M1–M5, mirrors; QWP, quarter-wave plate; Br, receiver beam splitter; Ms, steering mirror.

expansion, we determined beam coefficients for the laser at the primary lens of the telescope and applied the appropriate phase change. As Fig. 2 shows, there are multiple elements in the optical path. In determining the beam coefficients, we had to take into account each element that changes the shape of the beam, i.e., truncation or obscuration.

It is not possible to determine the beam coefficients after the primary lens by direct computation. The exact field profile is known at the laser, but it changes as the beam is propagated along the optical path. This change is caused by the changing phase relationship among the Hermite–Gaussian modes. As a result of the change, the exact field profile is unknown after the primary lens. For simplicity in calculating the beam coefficients, we assume the elements between the laser and the telescope to have no effect on the shape of the beam; expansion, collimation, and splitting of the beam are addressed by simple calculations on the reference beam. If the system is well aligned, the beam passes through the centers of the elements and is not appreciably truncated until reaching the telescope, as shown in Fig. 3.

As a result of this phenomenon, the only elements that affect the beam shape and beam coefficients are the wire and the telescope. The intermediate elements can be ignored, because after a beam passes through an aperture,

$$E_{\text{out}}(x, y) = E_{\text{in}}(x, y)P(x, y), \tag{19}$$

where

$$P(x, y) = \begin{cases} 1, & \text{if } (x, y) \text{ is inside aperture,} \\ & \text{not obscured,} \\ 0, & \text{if } (x, y) \text{ is otherwise.} \end{cases} \tag{20}$$

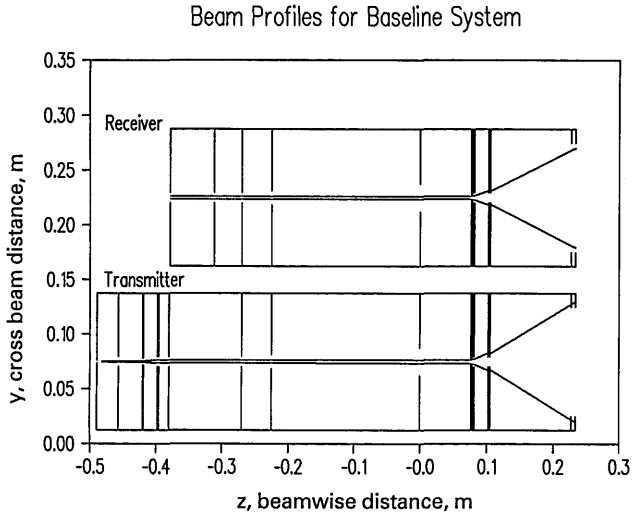

Fig. 3. Gaussian beam propagated through a laser radar. This figure shows how the size of the Gaussian beam changes as it propagates along both the transmitter and receiver (BPLO) paths. With proper alignment, neither the transmitter nor the receiver beams are truncated until reaching the secondary of the telescope, S.

The beam coefficients after the aperture are

$$\begin{aligned} A_{mn}^{(\text{out})} &= \int\int E_{\text{out}}(x, y)h_{mn}(x, y)\text{d}x\text{d}y, \\ &= \int\int \sum_k \sum_l A_{kl}^{(\text{in})} h_{kl}(x, y)h_{mn}(x, y)\text{d}x\text{d}y, \\ &= \sum_k \sum_l A_{kl}^{(\text{in})} \int\int h_{kl}(x, y)h_{mn}(x, y)\text{d}x\text{d}y, \\ &= \sum_k \sum_l A_{kl}^{(\text{in})} C_{klmn}, \end{aligned} \tag{21}$$

where

$$C_{klmn} = \delta_{km}\delta_{ln} \tag{22}$$

for an infinite aperture, or an aperture that is at least larger than the beam size with no obscuration. Therefore, if the aperture is larger than the beam, i.e., the beam is not truncated,

$$A_{mn}^{(\text{out})} = A_{mn}^{(\text{in})}, \tag{23}$$

and it is justified to ignore the optical elements between the laser and the wire in determining the final set of beam coefficients. For simplicity the wire and the telescope are taken to be a single element with regard to the determination of the beam coefficients. This is a valid assumption because the phase change in going from the secondary to the primary of the telescope is only a few degrees, because the beam is sufficiently diverged so that geometric optics is a good approximation and diffraction effects are small. With these assumptions made, the process of determining the beam profiles after the primary lens consists of the following:

- Determining the beam coefficients at the laser,
- Computing beamwidth and phase at the wire and telescope
- Determining the beam coefficients at the primary,
- Determining the beam profiles at different ranges from the primary.

Beam Coefficients

In this system, the transmitter beam has a square-bore width of 2 mm. Therefore, w in Eq. (1) is taken to be 1 mm. Using Eq. (2), we determined a set of transmitter-beam coefficients for the output of the laser.

To determine the beam coefficients at the primary of the telescope, we must know the radius of the beam with respect to the primary and the phase change of the beam. In determining the beam coefficients, we fit the beam profile to a Gaussian beam with a radius of 0.7 mm to maximize the power in the 00 order. According to the properties of Gaussian beams, this reference Gaussian beamwidth will change as it propagates from the laser along the optical path to the wire and telescope. The Gaussian beam radius at the primary is 35 mm, and the phase change is 95.5°.

The radius of the primary is 50 mm, so the ratio of the beamwidth to the primary is 7:10.

The wire is centered on the x axis and has a width that is one eighth of the diameter of the aperture. The beam coefficients were then determined by Eq. (2), taking the integration over the primary lens with the electric field determined as mentioned above, except over the wire, where the electric field was taken to be zero.

SNR and Beam Profiles

The transmitter and BPLO beam coefficients are assumed to be identical for simplicity. This assumption is valid because the path lengths are nearly the same, so the beam size and phase are close. By determining the beam-profile efficiency as a function of range, we can determine the actual SNR by correcting the results obtained by modeling the system as matched Gaussian beams[4] of size $D = 100$ cm.

The beam-profile efficiency was calculated as a function of range (distance from the telescope). The actual SNR was then determined by appropriately scaling the previous results[4] according to the resulting beam-profile efficiencies. For these calculations the focus was taken to be at 2 m. Figure 4 shows the actual SNR as a function of range compared with the nominal SNR[4] and the SNR as determined by modeling the system using a truncated Gaussian.[8] The SNR calculation was based on the power measured before the telescope and thus does not take into account losses incurred during the two-way travel of the beam through the telescope. As Fig. 4 shows, the actual SNR is nearly 10 dB lower at the focus than that for the matched Gaussian case and 5 dB lower than the truncated Gaussian case. Figure 5 compares the theoretical SNR for the system and the experimentally measured SNR. As Fig. 5 shows, the

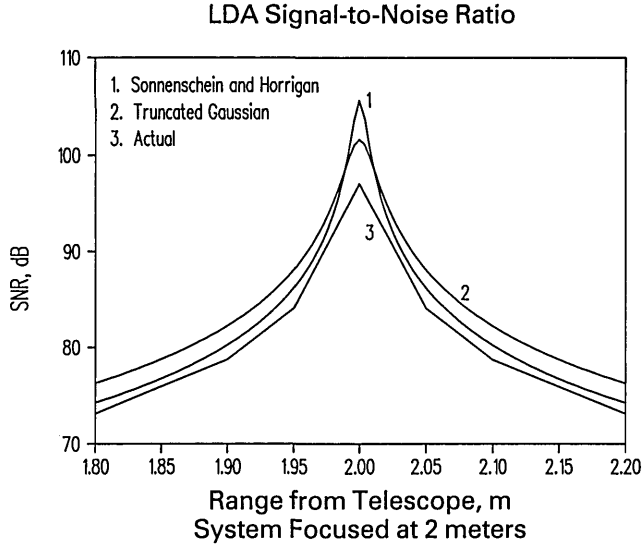

Fig. 4. Theoretical SNR for the laser radar system as a function of range from the target using different solutions: 1, matched Gaussians; 2, truncated Gaussian; 3, obscured and truncated Gaussian.

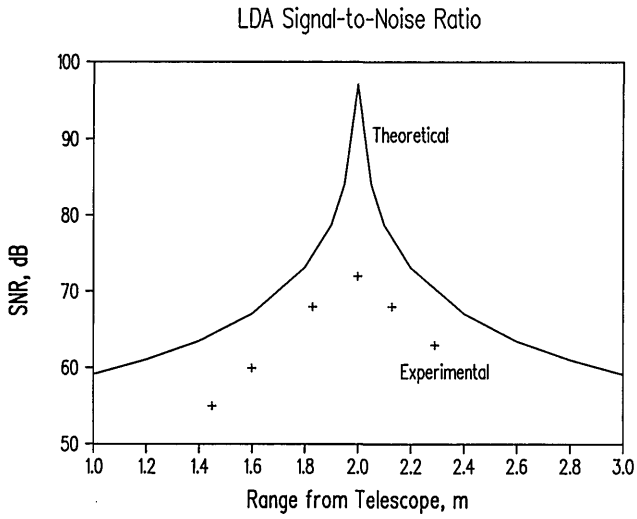

Fig. 5. Experimental versus theoretical SNR for a laser radar system as a function of range from the telescope. The theoretical SNR is based on an obscured and truncated Gaussian.

experimental SNR is much lower than the theoretical SNR at the focus. Other measurements have shown that 10–12 dB of this loss can be accounted for by the system before the telescope, caused by optical losses and misalignment. Another 4 dB can be accounted for by the loss caused by reflection from the optics in the telescope. The measured SNR and the theory differ by approximately 10 dB after these losses are taken into account. This loss may be accounted for by further misalignment of the optical system.

Once the coefficients for the output beam were determined, the beam profile could be determined for any range from the primary by making the appropriate phase change. For the beam-profile experiment, the telescope was adjusted to focus the beam to a range of approximately 18.5 m. This range was chosen because it provided an adequate spot size at the focus for photographic measurements.

If the radius of curvature of the Gaussian beam at the primary lens is taken to be -18.5 m with the CO_2 wavelength of 10.6 μm, the distance from the focus to the primary is 18.45 m and the Rayleigh range $b = 0.940$ m. Rearranging the Rayleigh range equation, we determine the Gaussian beamwidth at the beam waist to be

$$d_0 = \sqrt{4\lambda b/\pi} = 3.56 \text{ mm}. \tag{24}$$

To determine the beam profile for any range, we find that the phase change to the second set of beam coefficients is

$$\psi = (1 + m + n)\tan^{-1}\{[z - 18.45]/0.940\}, \tag{25}$$

where z is the distance from the primary of the telescope.

The beam profiles for various distances from the waist were photographed. The CO_2 wavelength is not in the visible spectrum, so the profiles could not be photographed directly. We photographed them

by letting the beam fall on ultraviolet blocks of the appropriate sensitivity. These blocks fluoresce in the yellow when illuminated by ultraviolet light, but this fluorescence is quenched by infrared light, creating a black spot in the shape of the infrared beam profile, thus permitting the profile to be photographed. The actual profiles and the corresponding profiles resulting from the beam coefficients are displayed in Fig. 6.

From the actual beam profiles, it appears that the beam is not passing through the center of one or more elements in the optical path. This phenomenon is shown by the asymmetric properties displayed by the beam profiles. This asymmetry is a result of the misalignment of the beam. From the profile in Fig. 6(c), it appears that the beam is being clipped by an optical element or holder. However, even with the lack of symmetry displayed by the profiles, there is a good agreement with the profiles determined from the Hermite–Gaussian expansions. The computed beam profiles compare quite favorably with the upper halves of the actual beam profiles for measurements taken before the focus. For measurements taken after the focus, the lower halves compare favorably with the computed profiles.

The beams shown in Figs. 6(a) and 6(b) are good matches with their respective computed profiles, although because of the misalignment, one of the sidelobes is darker than the other. In Fig. 6(a), which is the measurement taken at or near the focus, the separation of the sidelobes is evident in the computed profile. From the computed profiles we find that the sidelobes should be approximately 3.5 mm from the mainlobe. In the actual profile we see that the upper lobe is 4.7 mm from the mainlobe and that the lower lobe is nearly 3.5 mm from the mainlobe. Assuming that the misalignment of the system caused the lower half of the beam profile to be inconsistent, we would conclude that this measurement was not taken at the exact focus, but slightly beyond. This conclusion is based on the fact that the profile appears to have inverted as it should when passing through the focus. In Fig. 6(b), clearly beyond the focus, the sidelobes have started to get closer to the mainlobe and the mainlobe is starting to spread out. The shape of the computed profile is in agreement with this observation. In addition, the lower lobe is 3.4 mm from the mainlobe as compared with 3.6 mm in the computed profile.

The beams in Figs. 6(c) and 6(d) are separated only a few degrees in phase, so their profiles have not changed a great deal. At these distances the separation between the sidelobes and the mainlobe is negligible. Of particular interest is the fact that the sidelobes are getting stronger as the beam moves toward the focus. This observation agrees with the computed profiles. Also of interest is the distance between the center of the mainlobe and the center of the upper lobe. In Fig. 6(c) the actual distance is 3.5 mm and the computed distance is 3.4 mm. In Fig. 6(d) the actual distance is 4.7 mm and the computed distance is 4.6 mm.

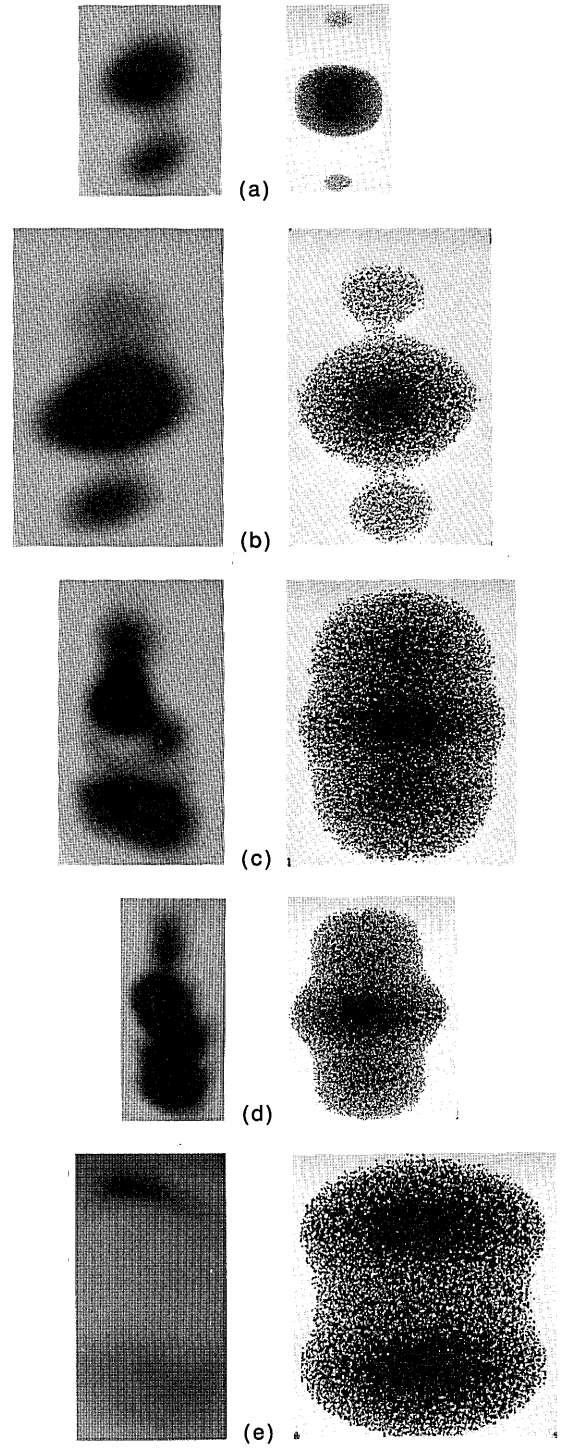

Fig. 6. Actual versus computed beam profiles for transmitter beams: (a) z = 18.45 m, ψ = 87.1°; (b) z = 19.95 m, ψ = 142.9°; (c) z = 15.35 m, ψ = 13.8°; (d) z = 14.05 m, ψ = 9.2°; (e) z = 12.35 m, ψ = 5.9°. The computed profiles have a 10-dB dynamic range.

The last measurement, displayed in Fig. 6(e), was the closest measurement to the telescope. The difference between the theoretical and experimental profiles could be the result of one of two things. First,

the intensity of the beam for this measurement is lower because the power is spread out over a larger area. As a result, the strength of the infrared profile was reaching the lower limit of the sensitivity of the ultraviolet block, so low power in the center of the beam may have been undetectable on the ultraviolet block. Second, the difference may be caused by the theoretical beam profile. For any type of obscuration many terms are needed in the expansion, because of the high-frequency terms related to the abrupt cutoff of the profile. Therefore, more terms may be needed to get the profile, but not the SNR.[1] The ultraviolet-block sensitivity seems to be the more likely cause of the difference, because considering the distance between the two lobes, the two profiles are in good agreement. The two lobes are 6.7 mm apart in the actual profile and 5.8 mm apart in the computed profile.

Summary

The SNR equations for a heterodyne laser radar have been presented. The equations are applicable to all types of laser radar: focused, unfocused, cw, and pulsed systems. Also presented was the concept of the beam-profile efficiency, $\eta_{BP}(R)$, and a comparison with system efficiencies as defined by other authors. To optimize a system design in the far field, we must maximize either η_s or η_{BP}. To optimize in the near field, we must maximize the beam-profile efficiency. In optimizing the system design, this quantity takes into account any truncation or obscuration of the transmitter and BPLO beams, any diffraction of the transmitter and BPLO beams, and the coherence between the local oscillator and the return signal.

There are a number of ways to evaluate the beam-profile efficiency. Fresnel–Kirchhoff integrals are commonly used, as is the method of expanding the laser-beam profile as a sum of orthogonal functions. When expanding the laser-beam profile, we find that two of the most promising choices appear to be Hermite–Gaussian functions for beam profiles with rectangular symmetry, and Laguerre–Gaussian functions for beam profiles with circular symmetry.

The method employed to evaluate the beam-profile efficiency is a matter of personal choice. However, the beam-profile efficiency is the quantity that must be maximized to ensure the highest possible SNR for a laser radar system. Hermite–Gaussian functions are useful because the lowest-order terms contribute the most to the signal.[1] Therefore, only a few terms are required to obtain the SNR.

References

1. C. A. DiMarzio and C. S. Lins, "Heterodyne SNR computations using orthogonal functions," in *Fifth Conference on Coherent Laser Radar: Technology and Applications,* J. W. Bibn and C. Werner, eds., Proc. Soc. Photo-Opt. Instrum. Eng. **1181,** 176–185 (1989).
2. R. G. Frehlich, "Atmospheric refractive turbulence and coherent laser radar performance," in *Coherent Laser Radar: Technology and Applications,* Vol. 12 of OSA 1991 Technical Digest Series (Optical Society of America, Washington, D.C., 1991), paper TuB3.
3. B. J. Rye and R. G. Frehlich, "The truncated Gaussian lidar antenna problem revisited," in *Coherent Laser Radar: Technology and Applications,* Vol. 12 of OSA 1991 Technical Digest Series (Optical Society of America, Washington, D.C., 1991), paper WA6.
4. C. M. Sonnenschein and F. A. Horrigan, "Signal-to-noise relationships for coaxial systems that heterodyne backscatter from the atmosphere," Appl. Opt. **10,** 1600–1604 (1971).
5. H. Koglnik and T. Li, "Laser beams and resonators," Proc. IEEE **54,** 1312–1329 (1966).
6. A. Siegman, *Lasers* (University Science Books, Mill Valley, Calif., 1986).
7. M. Abramowitz and I. Stegun, *Handbook of Mathematical Functions* (National Bureau of Standards, Washington, D.C., 1964).
8. R. M. Huffacker, H. B. Jeffreys, E. A. Weaver, J. W. Bilbro, G. D. Craig, R. W. George, E. H. Gleason, P. J. Marerro, E. J. Reinbold, and J. E. Shirey, "Development of a laser Doppler system for the detection, tracking, and measurement of aircraft wake vortices," Rep. FAA-RD-74-213 (Federal Aviation Agency, Washington, D.C., 1975).